The Thesis committee for Kevin Arthur Jumper

Certifies that this is the approved version of the following thesis:

Do Metal-Polluted Stars of the ZZ Ceti Instability Strip Have A Distinct Asteroseismic Signature?

APPROVED BY

SUPERVISING COMMITTEE:

Don Winget, Supervisor

Mike Montgomery, Co-Superivsor

Chris Sneden

Do Metal-Polluted Stars of the ZZ Ceti Instability Strip Have A Distinct Asteroseismic Signature?

by

Kevin Arthur Jumper, B.S.

Thesis

Presented to the Faculty of the Graduate School

of the University of Texas at Austin

in Partial Fulfillment

of the Requirements

for the Degree of

Master of Arts

The University of Texas at Austin

August 2015

Dedication

This thesis is dedicated to my family, for nurturing my love of science and supporting my endeavors throughout the years.

Acknowledgements

I acknowledge the financial support of the University of Texas at Austin and my research supervisors while I worked toward this Master's Thesis. I also thank the staff of McDonald Observatory for helping instruct me in the proper use of telescopes and the members of the Central Texas Astronomical Society, particularly Dean Chandler, Aubrey Brickhouse, and Willie Strickland, who made it possible for me to use Meyer Observatory in June 2014. Additionally, I thank Keaton Bell for observing WD 1145+288 on my behalf and for his technical and programming advice, and Sam Harrold, who provided further assistance on such matters. I also thank Barbara Castanheira for directing me to several references that were helpful for conducting my archival analysis. Lastly, I thank my undergraduate adviser, Dr. Robert Fisher, for helping guide me on my path to UT Austin.

Do Metal-Polluted Stars of the ZZ Ceti Instability Strip Have A Distinct Asteroseismic Signature?

by

Kevin Arthur Jumper, M.A.

The University of Texas at Austin, 2015

Supervisors: D.E. Winget, Mike Montgomery

Cooling DA stars that pass through the ZZ instability strip, a region between temperatures of approximately 12,600 K to 11,100 K, tend to experience the driving of g-mode pulsations near their surface layers. These pulsations cause variations in the luminosities of such stars, leading them to be known as DAVs. A fraction of DAVs also have photospheres contaminated by metals, usually thought to be from the tidally disrupted remnants of planetary systems. The high resolution spectroscopy needed to make definite identifications of these metal lines is relatively demanding, whereas it is simple to obtain photometric data on the pulsation periods of DAV stars. Therefore, if known metal-polluted DAVs (DAZVs) have systematic differences in their photometric data compared to that of DAVs that lack such pollution, photometry could provide an easy way to determine which stars are likely to contain metals in their photospheres in the future. However, we find that the known DAZV population is not large enough to permit its behavior to be distinguished from that of the normal DAV population at the present time, though extremely low-mass white dwarfs may help expand the populations and improve the quality of our fits.

Table of Contents

List of Tables

List of Figures

1 Introduction

1.1 The ZZ Ceti Instability Strip, Pulsations, and Photometry

Approximately 80% of white dwarfs are DA stars (Kleinman et al. 2013; Hermes et al. 2013b), meaning that their atmospheres are dominated by hydrogen. Like other white dwarfs, DAs slowly cool over billions of years, and as their temperatures become low enough they will enter a region of the HR diagram called the ZZ Ceti instability strip, in which the stars' hydrogen partial ionization zones are situated at suitable depths to facilitate the convective driving of nonradial gravity modes (g-modes) across their surfaces, via the mechanism described by Brickhill (1991). A crucial condition for this to occur is that the timescale of convective overturning must be shorter than the timescale of turbulent perturbations (Brickhill 1991). The regular generation of g-modes has the effect of causing periodic changes in a star's luminosity, which renders pulsating stars photometrically detectable based on this variability (Carroll & Ostlie 2007). Therefore, such pulsators are called DA variables, hereafter abbreviated as DAVs.

The estimated boundaries of the ZZ Ceti instability strip have been revised on numerous occasions in light of new empirical data and revised stellar atmosphere models. Two recent estimates for the hot, or blue, edge of the strip are roughly 12300 K (Castanheira et al. 2013) and 12,600 K (Hermes et al. 2013b), while corresponding estimates for the cool, or red, edge of the strip are 10500 K (though pulsations will cease closer to 11,000 K for normal mass white dwarfs)

and 11,100 K. And the strip's boundaries continue to be revised; more recent 3-D convection calculations led Tremblay et al. to believe that both edges may be pushed downward in temperature (2013).

The first known DAV star was HL Tau 76, which was identified as a pulsator in 1968 (Landolt 1968). Today, we know of over 150 DAVs (Castanheira 2010; 2013) or even up to about 160 (Castanheira 2014). Collectively, the pulsation modes of these stars, as determined by time series photometry and Fourier analysis, provide a wealth of data about the interiors of DAVs through the study of asterosiesmology, making them of significant interest to the community.

1.2 Metal Pollution

Another property of white dwarfs that is of interest to astronomers is that a fraction of them have photospheres that are contaminated with metals; metal-polluted DA stars are henceforth referred to as DAZs. An early known example of a DAZV is G29-38, which was discovered to have an excess in its infrared spectrum, indicative of the reradiation of energy from metals in a surrounding debris disk (Zuckerman & Becklin 1987). Further studies of metal-polluted spectra have shown that DAZVs have a similar bulk composition to Earth and our solar system's other terrestrial planets and asteroids, suggesting that the metals may have originated from tidally disrupted planets and asteroids that existed around such DAZs (Jura 2012; Zuckerman et al. 2010), making DAZs popular targets for planetary astrophysicists.

Debris disks have been observed around 2.6% to 4.1% of single white dwarfs (Barber 2014), but not all DAZs that have been discovered so far have detectable debris disks. Indeed Kilic and Redfield (2007) estimate that as few 14 % percent of DAZs may actually have such infrared excesses, and Jura (2008) hypothesizes that only larger tidally-disrupted bodies will actually form a detectable disk, while smaller asteroids will accrete onto the star without producing a significant infrared excess.

In any case, matter must be accreted at an average rate of approximately $10^6 \mathrm{gs}^{-1}$ in order for metal lines to be spectroscopically detectable (Debes et al. 2012). This is in large part because metals sink out of the white dwarf photosphere through gravitational settling, and, more importantly, electrical diffusion, on timescales of a few days to weeks for most species (Koester & Wilken 2006), meaning that they would disappear without the stars steadily accreting new metallic material. Given such considerations, Debes et al. (2012) estimated that about 30% of white dwarfs should have visible metal lines.

Considering further estimates of the total fraction of metal pollution in the DA population, an early estimate by Zuckerman et al. (2003) based on HIRES spectroscopy found that about 25% of single cool white dwarfs had significant metal pollution, and Zuckerman et al. later estimated on account of infrared observations that about 30% of the stars studied likely had planetary systems during their main sequence phases (2010), which is consistent with Debes et al.'s estimate. In a more recent survey of 85 hot DA stars, with temperatures between

17,000 K and 27,000 K, 56% of the sample showed evidence of metals and of these it was determined that at least 27% needed accretion to be occurring to maintain those metals in their photospheres (Koester 2014). While this sample of stars was significantly hotter than those in the ZZ-Ceti instability strip, and the presence of some of the metals observed in the hotter stars can be accounted for by radiative levitation (Koester 2014), the overall fraction of metal pollution also seems broadly consistent with those of the previous cooler studies.

2 Methodology

Presently, four DAZVs, each with an infrared debris disk, are known: G29-38, PG 1541+651, GD 133, and WD 1150-153 (Kilic 2014). Below, we discuss the known members of the DAZV class, as well as a star we formerly deemed to be a DAZV candidate, WD 1145+288, which has since been shown by our collaborator, Keaton Bell, to lack significant pulsations (Bell 2015). Subsequent subsections shall describe the selection of our DAV sample and methods for determining key white dwarf properties, such as effective temperature and log g, through spectroscopy and appropriate atmospheric models, as well as the importance of maintaining consistency in the models used within a sample.

2.1 Determination of Key White Dwarf Properties

2.1.1 Photometric Properties: Pulsation Periods

It is relatively simple to determine the photometric properties of a star, as these are based on the total light received from the star, and a CCD device, such as the ProEM camera, is sufficient for measuring this (Princeton 2012). With such an instrument, obtaining a light curve simply requires gathering a time series of frames that integrate the light incident upon the CCD over short exposure times, usually between 15 to 30 seconds. Of course, this method by itself does not give the pulsation mode periods that are of interest to asterosiesmology; one must follow up with Fourier analysis to identify the principle modes from the light curve. This

process is facilitated through the use of software such as Period 04 or a similar program.

Once the pulsation periods are known, there are a few ways in which we can characterize them. One method, as discussed in Mukadam et. al, is to calculate the weighted mean period of the stellar pulsations, hereafter referred to as the WMP (2006), as given below in Equation 1:

$$\mathrm{WMP} = \frac{\Sigma_{\mathrm{i}} \mathrm{P_i A_i}}{\Sigma_{\mathrm{i}} \mathrm{A_i}} \tag{1}$$

Here, P_i is an individual pulsation period with index i and A_i is its corresponding amplitude, while Σ_i retains its usual meaning of denoting summation over i.

Alternatively, one may instead choose to focus on the pulsation period with the largest amplitude, which we'll refer to henceforth as the main period. Empirically, the amplitudes of the pulsation periods are seen to increase as a white dwarf cools until it gets close to the red edge of the instability strip, at which point the amplitudes will begin to drop off again (Mukadam et al. 2006).

2.1.2 Spectroscopic Properties: Effective Temperature and log g

In contrast to a star's pulsation periods and amplitudes, it is impossible to determine a star's effective temperature, which tells us whether it rests within the ZZ Ceti instability strip or not, from time series photometry alone; spectroscopy must be used in conjunction with appropriate atmosphere models. Likewise, log

g, which corresponds to the mass of the star, is estimated from the broadening of spectral lines.

However, there are several complications in estimating these quantities. Firstly, interpreting the Balmer lines of ZZ Ceti stars has long been problematic to observers, as they tend to be around their maximum strength in the temperature range of the instability strip and are thus relatively insensitive to model parameters in this regime (Koester & Allard 2000). Moreover, models still resort to the mixing-length theory of convection, which is merely a parameterization which mocks up poorly-understood phenomena while attempting to remain as self-consistent as possible, making it highly dependent on the known constitutive physics (Koester & Allard 2000; Gianninas et al. 2011). And given observational limitations and gaps in the constitutive physics, the uncertainties in these models remain significant. For example, when Gianninas et al. switched from a $ML2/\alpha = 0.6$ formulation of mixing length theory to $ML2/\alpha = 0.8$ mixing length theory in light of new information on Balmer lines and Stark broadening, the estimated effective temperatures of many stars shifted by a few hundred Kelvin (Tremblay & Bergeron 2009; Tremblay et al. 2010; Gianninas et al 2011).

Uncertainties such as these and the evident model-dependence of estimates for effective temperature and log g underscore the importance of using a single model when comparing the properties of DAV stars to maintain self-consistency in the sample (Mukadam et al. 2006). Fortunately, each of the confirmed DAZVs can be found within the results of Gianninas, Bergeron, and Ruiz's spectroscopic

survey (2011), which itself used stars selected from McCook and Sion's earlier survey (1999). McCook and Sion's sample contains, among other white dwarfs, approximately 1100 DA stars, though only 49 of these are both within the temperature range of the ZZ Ceti instability strip and actually pulsate (1999). While this is but a fraction of the total known DAV population, currently around 150-160 stars (Hermes et al. 2013a; Castanheira et al. 2013, Castanheira et al. 2014), we must exclude the others for the aforementioned reasons of self-consistency.

2.2 3-D Convection Corrections

A shortcoming to Gianninas et al.'s approach is that their model atmosphere models were one-dimensional in nature, which necessarily sacrifices some accuracy for a three-dimensional phenomenon such as convection (2011). Tremblay et al. addressed this problem by running grids of three-dimensional convection models over a wide range of physical conditions [$6000 < \mathrm{T_{eff}(K)} < 15000$ and $7 < \log(\mathrm{g})[\mathrm{cgs}] < 9$] (2013). They found that the 3-D results were less sensitive to the parameterization than the 1-D case, but that nonetheless, values between $ML2/\alpha = 0.7$ and $ML2/\alpha = 0.8$ produced the best results, which is generally consistent with Gianninas et al.'s previous use of $ML2/\alpha = 0.8$ (Tremblay et al. 2013). Indeed, Tremblay et al. frequently refer back to Gianninas et al.'s 2011 sample as a basis for their calculations within the regime of the ZZ Ceti instability strip and find that when the 3-D model is applied the effective temperatures and log g values of the stars decrease compared to those found by Gianninas et al. 2011 (2013).

Conveniently, Tremblay et al. provide analytic fits for converting between 1-D and 3-D values for effective temperature and log g (2013). We reproduce these fits for the $ML2/\alpha = 0.8$ case below in equations 2-5.

$$g_X = \log(\mathrm{g})[\mathrm{cgs}] - 8.0 \tag{2}$$

$$T_X = \frac{T_{\mathrm{eff}}(\mathrm{K}) - 10000}{1000} \tag{3}$$

$$\frac{\Delta T_{\mathrm{eff}}}{1000} = c_o + (c_1 + c_6 T_X + c_7 g_X)\exp[-\mathrm{c_2} + \mathrm{c_4 T_X} + \mathrm{c_5 g_X})^2(\mathrm{T_X} - \mathrm{c_3})^2] \tag{4}$$

$$\begin{aligned} \Delta\log(\mathrm{g}) = (\mathrm{d_0} + \mathrm{d_4}\exp[-\mathrm{d_5}(\mathrm{T_X} - \mathrm{d_6})^2]) + \\ d_1 \exp\left(-\mathrm{d_2 T_X}(\mathrm{d_3} + \mathrm{d_7}\exp(-[\mathrm{d_8} + \mathrm{d_{10} T_X} + \mathrm{d_{11} g_X}]^2[\mathrm{T_X} - \mathrm{d_9}^2))]^2\right) \end{aligned} \tag{5}$$

The constants for the effective temperature fit (Equation 4) are given in Table 1, while those for the log g fit (Equation 5) are given in Table 2.

We will report both the original 1-D values taken from Gianninas et al. (2011) and the converted 3-D values that we will use for our final fits.

2.3 The Known DAZVs and Candidates

Having defined our sample and the 3-D convection conversion that we will be using, let us now consider the properties of the known DAZV stars and WD 1145+288.

c_o	1.0947335×10^{-3}
c_1	$-1.8716231 \times 10^{-1}$
c_2	1.9350009×10^{-2}
c_3	6.4821613×10^{-1}
c_4	$-2.2863187 \times 10^{-1}$
c_5	5.8699232×10^{-1}
c_6	$-1.0729871 \times 10^{-1}$
c_7	1.1009070×10^{-1}

Table 1: Constants from the fit converting effective temperatures determined with 1-D convection to corresponding values for 3-D convection, as found in Tremblay et al. 2013.

d_o	7.5209868×10^{-4}
d_1	$-9.2086619 \times 10^{-1}$
d_2	3.1253746×10^{-1}
d_3	$-1.0348176 \times 10^{-1}$
d_4	6.5854716×10^{-1}
d_5	4.2849862×10^{-1}
d_6	$-8.8982873 \times 10^{-2}$
d_7	1.0199718×10^{1}
d_8	4.9277883×10^{-2}
d_9	$-8.6543477 \times 10^{-1}$
d_{10}	3.6232756×10^{-3}
d_{11}	$-5.8729354 \times 10^{-2}$

Table 2: Constants from the fit converting effective temperatures determined with 1-D convection to corresponding values for 3-D convection, as found in Tremblay et al. 2013.

2.3.1 G29-38

G29-38, also known as WD 2326+049, was the first known example of a DAZV, shown to be variable in 1974 (Shulov & Kopatskaya), discovered to have an infrared excess in 1987 (Zuckerman & Becklin 1987; Graham et al. 1990) and proven to have Ca, Mg, and Fe contamination in its photosphere in 1997 (Koester et al. 1997). Moreover, as one of the best-studied DAVs, G29-38 has been found to have a rich array of pulsation modes (Mukadam et al. 2006; McGraw & Robinson 1975; Kleinman 1995). Putting these periods into equation 1 gives a WMP of 719.2 seconds, while G29-38's main period is 614.4 seconds and has an amplitude of 32.8 mma. Gianninas et al.'s model (2011) found an effective temperature of 12,220 K and a log g value of 8.22, which converts to 11910 K and 8.17, respectively, when Tremblay et al.'s (2013) corrections are taken into account.

2.3.2 WD 1150-153

Kilic et al. predicted that WD 1150-153 would display a debris disk in 2006 on account of its observed calcium lines (Kilic et al. 2006) and a follow up to this study detected an infrared excess, making it the second known DAV with such a feature (Kilic & Redfield 2007). Measurements of the pulsation periods also showed that WD 1150-153's main period is 249.6 seconds (Gianninas et al. 2006; Koester & Voss 2007) Kilic & Redfield 2007), and we can derive a WMP of 236.6 seconds. Gianninas et al. (2011) estimated the effective temperature of the star to be 12,637 K and log g to be about 8.22, which gives us 12441 K and 8.20 when

corrected for 3-D convection (Tremblay et al. 2013).

2.3.3 GD 133

GD 133, also known as WD 1116+026, was first identified as a pulsator in 2006 (Silvotti et al.), though it had previously been believed to be a non-pulsating star near the ZZ Ceti instability strip (Kepler et al. 1995). The presence of calcium in its atmosphere was initially detected by the SPY supernova progenitor survey (Koester et al. 2005), and since then a wider variety of metals, in proportions similar to bulk Earth, have been found in its photosphere (Xu et al. 2014), firmly classifying it as a DAZV. GD 133 has an effective temperature of 12599 K, log g of 8.12, a WMP of 123.5 seconds, and a main period of 120.4 seconds with an amplitude of 4.6 mma (Gianninas et al. 2011; Silvotti et al. 2006).

2.3.4 PG 1541+651

PG 1541+651 was identified by the Palomar-Green Survey (Green et al. 1986) and was determined to be a part of the ZZ Ceti Instability Strip by Vauclair et al. (2000). However, it was not until Kilic et al. discovered an infrared excess around the star that it was also known to have metals (Kilic 2012). PG 1541+651 has a WMP of 676.5 seconds, and a main period of 689 seconds with an amplitude of 45 mma (Vauclair et al. 2000). The 1-D effective temperature is 11880 K and the corresponding log g is 8.2 (Gianninas et al. 2011), which become 11559 K and 8.12 in the 3-D case (Tremblay et al. 2013).

2.3.5 Potential DAZV Candidate: WD 1145+288

Given the small size of the known DAZV population, we were interested in identifying new members of this class. Kilic suggested that we look at WD 1145+288 as a candidate DAZV; metals had been confirmed in its atmosphere, along with an effective temperature that would put it around the ZZ Ceti instability strip, 12290 K (12030K in the 3-D case), and it had a typical log g, 8.14 (8.10 when corrected for 3-D), for a normal-mass white dwarf, but there was no confirmation on whether it was variable or not (Kilic 2014; Barber et al. 2014; Tremblay et al. 2013). Consequently, we made plans to observe it at McDonald Observatory on the 82" telescope during the spring of 2015, when it would be visible in the sky.

2.4 Preliminary Observations

Additionally, we made plans to observe the known DAZVs GD 133 and PG 1541+651 to familiarize ourselves with basic telescope operation and gain an appreciation of the techniques of time series photometry. The former would be observed on the 36" telescope at MacDonald Observatory on the night of March 14, 2014, while the latter would be observed on the nights of June 27 to June 30 on the 24" telescope at the Central Texas Astronomical Society's (CTAS) Meyer Observatory. The GD 133 run did not have any particular scientific goals beside instruction as there was a nearly full moon on that night, which would add significant noise to the white dwarf's signal, while the PG 154+651 run would ideally verify the existence of the star's fourth pulsation mode, suggested by Vauclair

et al. (2000); the time for the latter was chosen to be around the new moon to maximize the darkness of the sky.

3 Results

3.1 Observations

3.1.1 Preliminary Observations

The GD 133 run accomplished its instructional objective of teaching us how to use a telescope. As for the PG 1541+651 run, there was significant cloud cover during the middle of the run, which made the data extremely noisy, and there were some technical issues with the camera's cooling mechanism, which caused delays or interruptions in the data each time it needed to be recalibrated. In spite of these difficulties, we obtained good quality data at the start and ends of the run, and additional data from Willie Strickland, the CTAS member who assisted us in operating the 24" telescope (Strickland 2014), and were able to practice reducing the data and running it through the pipeline to prepare it for analysis in Period 04. Of course, the main thrust of the project would be to conduct an archival study of the DAV population to see if stars polluted with metals behaved differently from those that were not polluted, so we eventually tabled further analysis of the new data from PG 1541+651 to focus on the former.

3.1.2 WD 1145+288

Prior to our planned run to observe WD 1145+288 in March, we realized that it would already be up in the sky during the January observing run of one of our colleagues, Keaton Bell. As observing this target would advance our research

group's overall interests, he observed this star on our behalf with the 82" telescope at MacDonald Observatory for a little over four hours on the night of January 18, 2015 (Bell 2015). Bell provided us with a Fourier transform of his light curve, which serves as Figure 1 below.

As we can see, there is plenty of noise, as would be expected from a Fourier transform of real measurements, but there are few frequencies that noticeably rise above the surrounding noise peaks - and none that do lie high enough above the noise for them to be identified as a true pulsation period at the 99% or 99.9% confidence levels, the later of which would require an amplitude of a little less than 2.7 mma (Bell 2015). Therefore, we tentatively conclude that that WD 1145+288 is not a DAV (Bell 2015); its periods, if they actually exist, lie at lower confidence levels.

Bell also took the opportunity to investigate another DAZ for variability on the subsequent night, WD 307+077, but following 3.5 hours of observations he found that there were no periods that had amplitudes above the desired confidence levels. For these observations, the 99.9% confidence level was located at an amplitude of 1.6 mma (Bell 2015).

3.2 Initial Checks

After gaining an understanding of the techniques underlying the data in our archival analysis, we performed a quick sanity check on our sample by reproducing Mukadam et al.'s fit for the ensemble properties of 39 ZZ Ceti stars (2006),

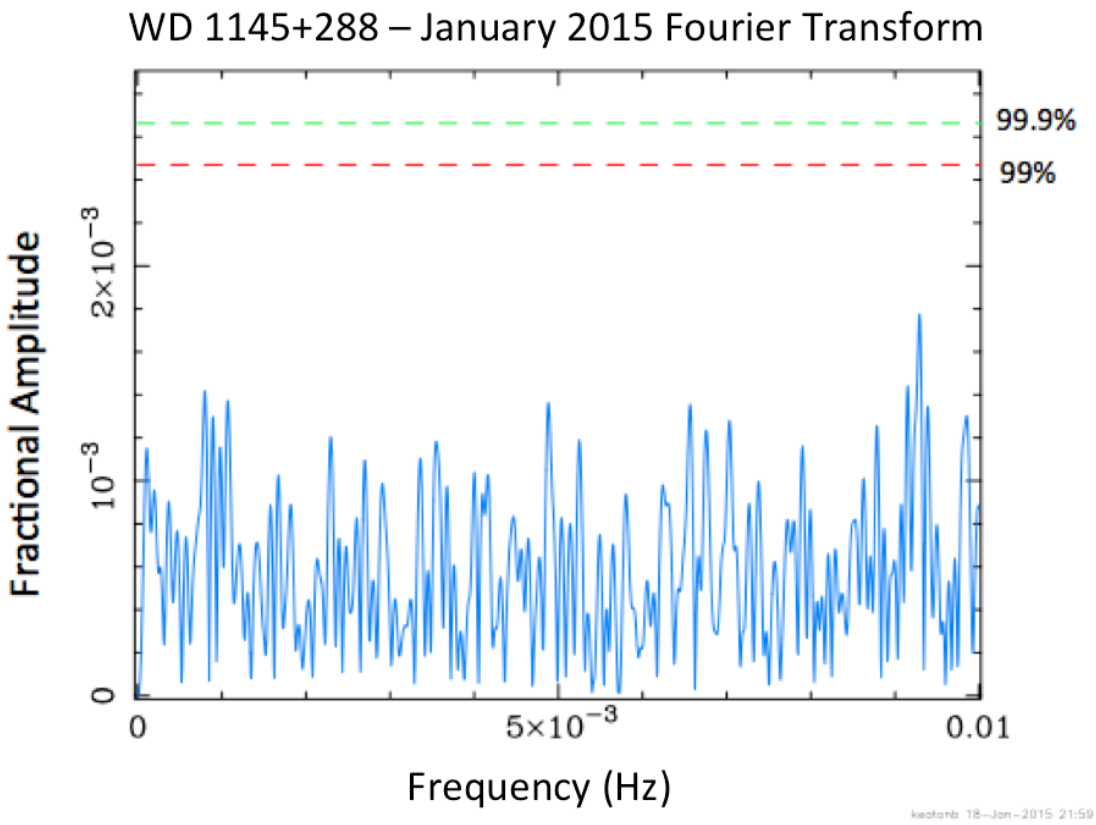

Figure 1: This is Bell's Fourier transform of WD 1145+288's light curve, as measured by Bell on the night of January 18, 2015. The horizontal axis is frequency in units of Hz, while the vertical axis gives the amplitude of the signal: each 10^{-3} here corresponds to 1 mma. The dotted lines indicate confidence levels; for instance, the green line is the 99.9% confidence level for the signal representing a genuine pulsation period, which corresponds to an amplitude slightly under 2.7 mma, while the red line is the 99% confidence level.

with the addition of three DAVs discovered since the publication of their paper, which had temperatures derived from Gianninas and Bergeron's older formulation of mixing length theory (Bergeron et al. 2004, Gianninas et al. 2005), as Mukadam et al. used these temperatures in their paper.

Mukadam et al.'s best fit line for WMP versus effective temperature is given below in Equation 6, and our updated version of this fit, which includes the four known DAZVs, is in Equation 7. We see that this fit is in good agreement with Mukadam's results, indicating that we have not made any egregious mistakes at this stage.

$$\mathrm{WMP}_{\mathrm{BG04}} = (-0.830 \pm 0.079)\mathrm{T}_{\mathrm{eff}} + (10,240 \pm 920) \tag{6}$$

$$\mathrm{WMP}_{\mathrm{check}} \approx (-0.830 \pm 0.094)\mathrm{T}_{\mathrm{eff}} + (10,260 \pm 1100) \tag{7}$$

Now let us consider the fit we obtain if we change the effective temperature estimates to those of a more modern model, first taking the results of the $\alpha = 0.8$ formulation of mixing-length theory of Gianninas et al. (2011) and then converting those values to those found in the case of 3-D convection (Tremblay et al. 2013). Let us also consider an additional five stars that were discovered since Mukadam et al.'s study and then find the resulting fit, which is given in Equation 8. We shall designate the subscript for this fit as "pop", standing for the total population of DAVs in our sample.

$$\mathrm{WMP}_{\mathrm{pop}} \approx (-0.59 \pm 0.07)\mathrm{T}_{\mathrm{eff}} + (7590 \pm 810) \tag{8}$$

Obviously, this best fit line is no longer consistent with the predictions of Mukadam et al., illustrating the dramatic effect that using a different method for calculating the effective temperatures can have (2006).

3.3 Comparison of the DAZV and Non-Metal Polluted DAV Samples

We can also consider the subsamples of the known DAZV and the non-metal polluted populations, which are given below in Equations 9 and 10 and shown alongside the population fit (Equation 8) in Figure 2.

$$\mathrm{WMP}_{\mathrm{DAZV}} \approx (-0.64 \pm 0.21)\mathrm{T}_{\mathrm{eff}} + (8200 \pm 2530) \tag{9}$$

$$\mathrm{WMP}_{\mathrm{not\ polluted}} \approx (-0.60 \pm 0.08)\mathrm{T}_{\mathrm{eff}} + (7620 \pm 880) \tag{10}$$

As seen above, we are presented with a problem: the uncertainties in the DAZV fit are quite large, leading to an accordingly broad confidence interval that completely encompasses that of the population which lacks metal pollution, meaning that we cannot rule out the possibility that these two fits are in fact the same. It also tells us that we will need a larger sample of DAZVs to reduce the uncertainties in its fit and narrow its confidence interval to a level more comparable to that of the normal population.

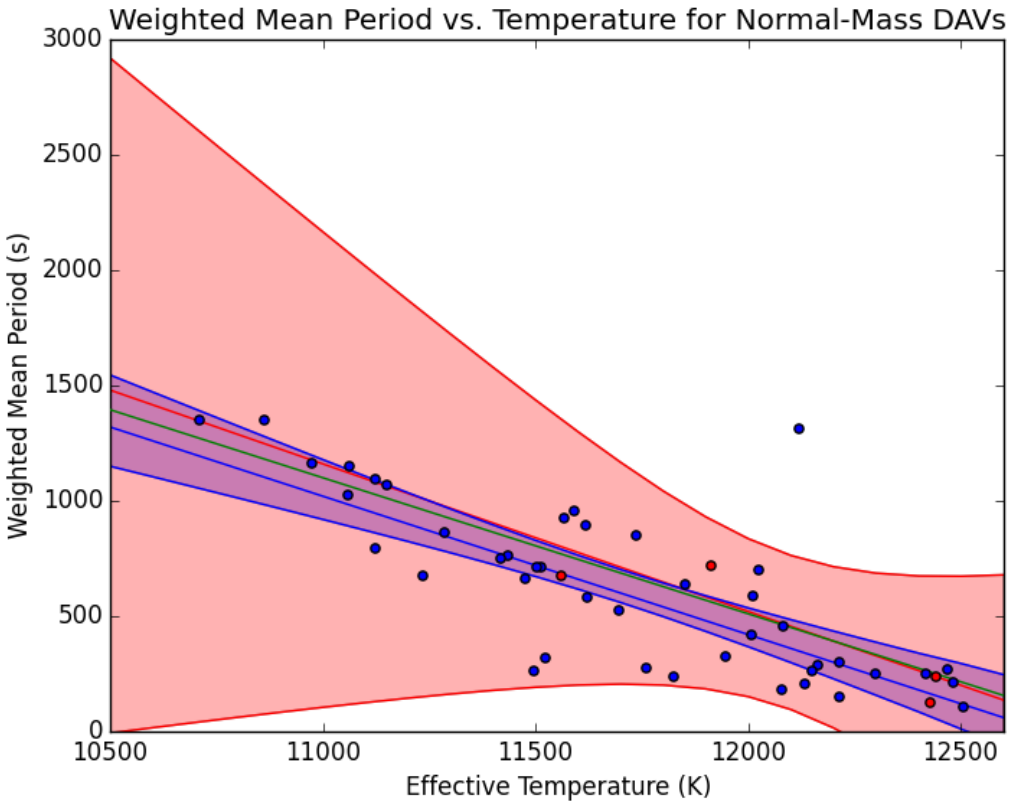

Figure 2: This figure shows the population fit (green), normal DAV fit (blue), and the DAZV fit (red) for WMP vs. effective temperature. We include 95% confidence intervals for the normal and the DAZV fits, which are shaded in their respective colors.

Now we repeat the above procedure, but this time fit the main periods against the effective temperatures, as illustrated in Figure 3 and equations 11-13 below.

$$P_{pop} \approx (-0.63 \pm 0.07)T_{eff} + (8010 \pm 850) \tag{11}$$

$$P_{DAZV} \approx (-0.61 \pm 0.14)T_{eff} + (7840 \pm 1660) \tag{12}$$

$$P_{not\ polluted} \approx (-0.64 \pm 0.08)T_{eff} + (8070 \pm 930) \tag{13}$$

Again, we find statistically indistinguishable populations. However, the uncertainties in the DAZV fits, while still large, have sharply decreased, while the uncertainties in the non-polluted DAV fit remain roughly where they were for the WMP fit.

Of course, this by itself does not say that other variables will fail to reveal differences between the populations. However, as we continued to study the relationships between other pairs of variables, much the same picture repeatedly emerged.

For instance, let us consider the results we obtain when we plot the main periods and their corresponding pulsation amplitudes against each other in Figure 4. A simple polynomial fit is less suitable in this case, but we observe the same qualitative behavior noted in Mukadam et al., namely increasing amplitudes with period to a point, after which the amplitudes begin to fall off once again (2006).

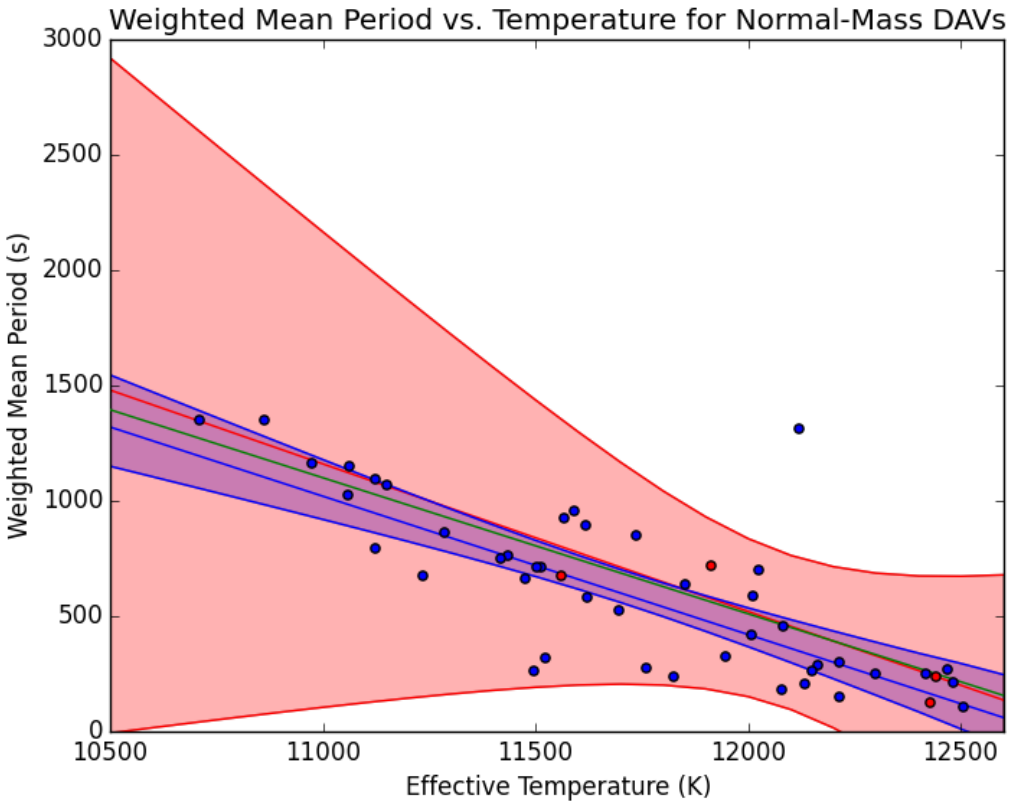

Figure 3: This figure shows the population fit (green), normal DAV fit (blue), and the DAZV fit (red) for main period vs. effective temperature. We include 95% confidence intervals for the normal and the DAZV fits, which are shaded in their respective colors.

At the same time, visual inspection does not show any obvious differences between the non-polluted DAV and DAZV populations.

We also briefly considered plots of the periods versus log g, which serves as a proxy for mass, as shown in Figures 5 and 6. We did not expect a significant difference to emerge, since the sample consisted of normal-mass white dwarfs, with log g values typically a little above 8, and within this range temperature is known to have a stronger effect on pulsation periods, though our advisor suggested checking it anyways in the interest of being thorough. However, there was predictably little difference between the periods for DAZVs and normal DAVs versus log g.

Lastly, let us consider the spectroscopically-derived properties of the DAVs, log g and effective temperature, given in Figure 7. We have already considered how each of the asterosiesmic variables compare to these, but it seems instructive to plot properties that most define the structure and behavior of DAVs together.

We see that log g is roughly constant with effective temperature. This is in line with our expectations, since the mass of the white dwarfs should not be changing significantly during the cooling process. And again, there are no obviously significant discrepancies between the populations.

While it is clear that there is no evidence for the asterosiesmic behavior of DAZVs being meaningfully different from non-metal polluted DAVs at this time, we will now procedure to a more detailed analysis of the significance of individual fits, sample sizes, and the possible contamination of our non-polluted sample with DAZVs.

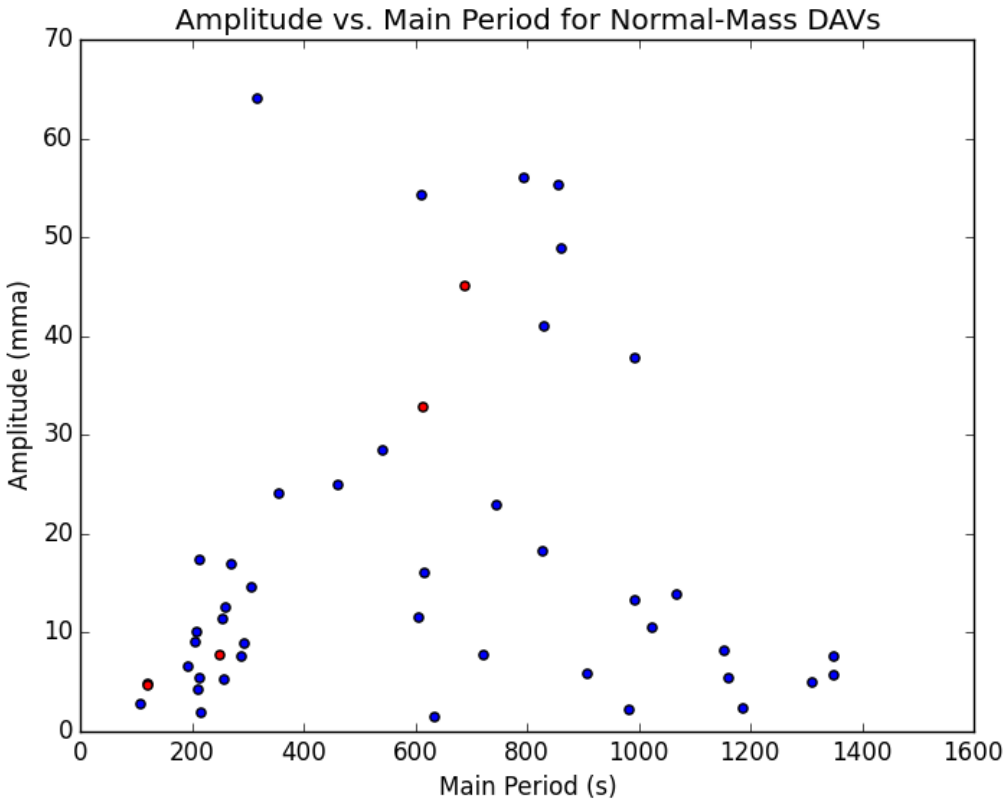

Figure 4: This figure shows the main periods of normal-mass DAVs on the horizontal axis and their corresponding pulsation amplitudes on the vertical axis. Known DAZV stars are marked in red, while stars that lack known metal pollution are in blue.

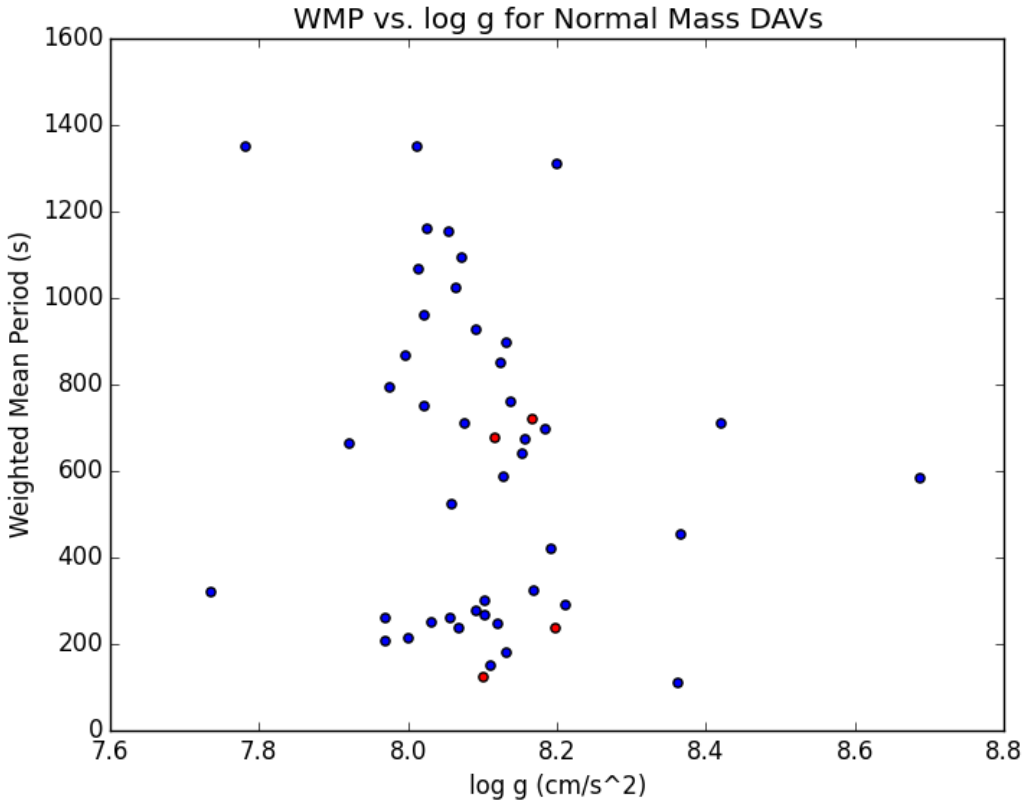

Figure 5: In this figure, log g is plotted on the horizontal axis, and the weighted mean period is on the vertical axis. Maintaining our previous convention, the known DAZVs are indicated by red points, while other DAVs are blue.

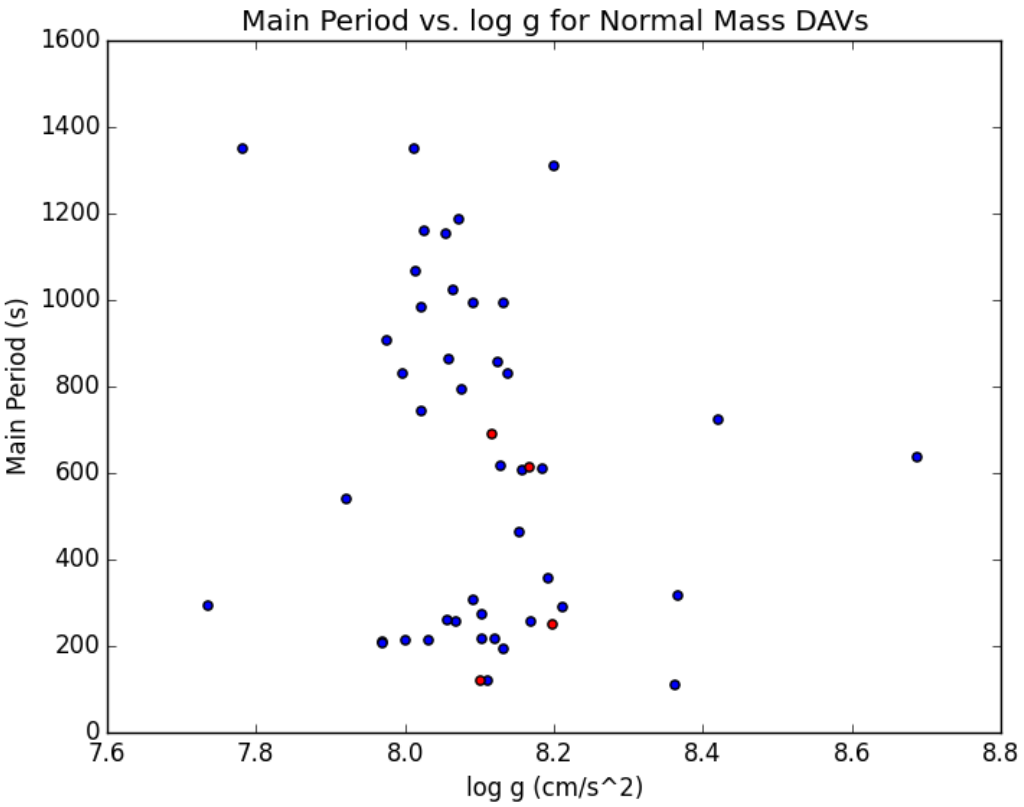

Figure 6: This figure follows the same conventions as Figure 5, except that the vertical axis now represents the main period of pulsation for each DAV.

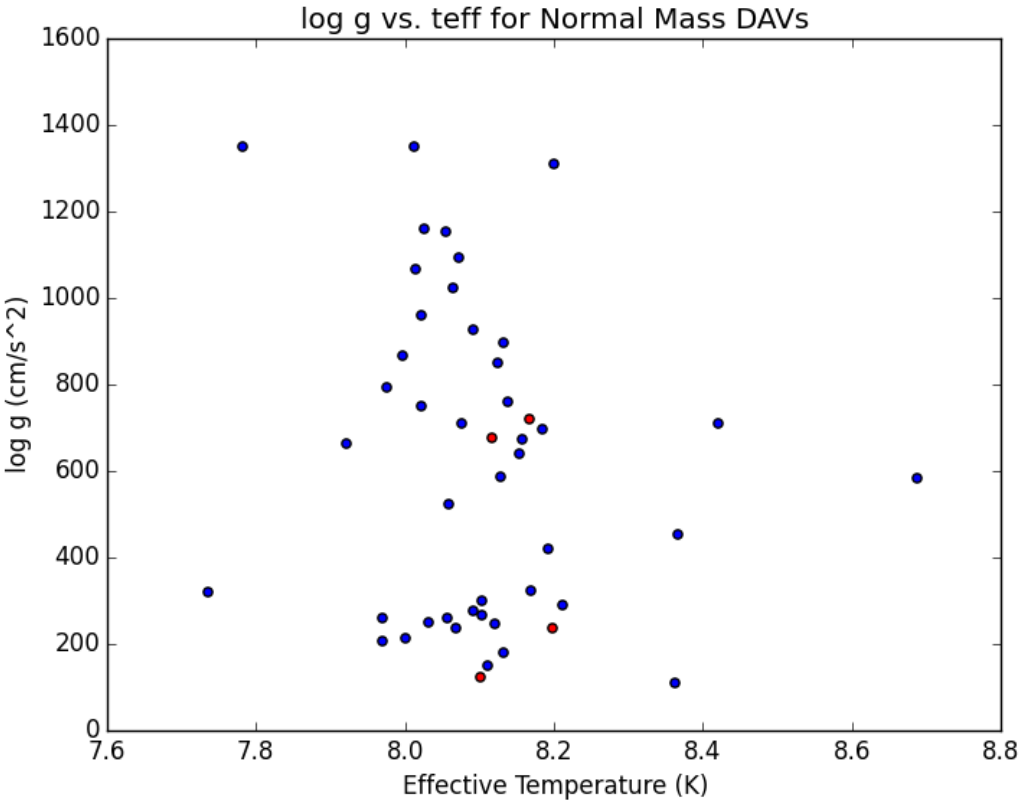

Figure 7: In this figure, effective temperature is on the horizontal axis and log g is on the vertical axis. As before, known DAZVs are in red, while other DAVs are in blue.

4 Discussion and Analysis

4.1 Quantifying the Significance of the Fits

We have seen in the preceding section that the uncertainties of the known DAZV fits overlap with those of the non-polluted population, but we would like to more precisely quantify their relationship.

Let us consider the slopes of the weighted mean period versus effective temperature lines for both the DAZV and non-polluted populations, and adopt the null hypothesis that the slopes of the two fits are identical. Carrying out our statistical analysis, we find that our p-value associated with this null hypothesis, the area under a normalized probability distribution for a measurement that is as or more extreme than the one observed, is ≈ 0.96. Typically in hypothesis testing, a value of 0.05 or less is considered to give significant evidence that the null hypothesis is incorrect. Given how lopsided this p-value is to the side larger than 0.05, the null hypothesis, that the slopes of the two lines are statistically the same, appears quite robust. We obtain a similar result, with $p \approx 0.98$ when we repeat the analysis for the main periods fit.

But what of the slope of the DAZV fit itself? Given its large uncertainties, we have cause to be concerned if it is actually significant or not. Let us assume a null hypothesis that the slope is equal to zero, that is there is no meaningful dependence between the weighted mean period and the temperature. In this case, we find $p \approx 0.09$. While not as lopsided as our previous test, it is still above

the 0.05 threshold needed for us to find significance. Moreover, the corresponding confidence interval for the slope is inclusive of zero. Therefore, the fit of WMP vs. effective temperature currently found for the DAZVs is not significant, and additional data points are needed so that significance can be achieved.

Interestingly, when we consider the significance of the slope of the main period vs. effective temperature fit, p drops to just a little under 0.05, making the fit marginally significant. Still, given the issues with the WMP vs. effective temperature fit and the tenuous significance of this one, our conclusion that a larger DAZV sample is needed remains unchanged.

4.2 Estimating An Appropriate DAZV Sample Size

As we have shown in the preceding subsection, the DAZV population is neither sufficiently large to be statistically meaningful nor to allow us to differentiate it from the stars that lack metal pollution. So how large of a sample are we likely to require?

If we consider the uncertainties in the fits, a simple way to address this question is to consider that the uncertainty in the mean value of a fit will tend to scale with $\frac{1}{\sqrt{N}}$, where N is the number of data points, given a certain amount of scatter in the data. So what must N be to keep the uncertainties surrounding the best values of the fits from overlapping?

Let us consider the fits of WMP vs. effective temperature, as these have larger uncertainties, and should thus necessitate a larger sample size to reduce the

uncertainties to a level at which the DAZV and non-polluted population could potentially be distinguished from each other and at which the DAZV fit itself could be found significant. The difference between the best values of the slope fits is approximately 0.04, and the uncertainty in the DAZV fit is about 0.20, while that of the non-polluted stars is about 0.08. There are many possible ways in which the uncertainties could be reduced so that they do not overlap, so for the sake of specificity, let us further consider the examples in which they are reduced to 0.02 for the DAZV and non-polluted fits, half of the current difference between the best fit values of the slopes. Following the $\frac{1}{\sqrt{N}}$ relationship for the uncertainty, this would imply 400 DAZVs or 188 non-polluted DAZVs.

Clearly, something is suspect with such a result, and in any case it would not be readily useful, given that it would require from several times to up to two orders of magnitudes more DAVs than are already known to be identified. The most obvious flaw is that with such a limited sample size of four stars for the DAZVs, we may not yet have an accurate measure of the scatter in the data, which may very well be less than that currently reported. Additionally, a more thorough analysis would simultaneously consider the effects of the uncertainties in the slope and intercept fits, which would constrain our results in a matter similar to the confidence intervals in Figures 2 and 3.

4.3 Contamination of the Non-Polluted Sample

As previously discussed in section 1.2, between 27-56% of the total DA population shows evidence of metal pollution (Zuckerman et al. 2010; Koester 2014). Yet currently, only 4 out of 47 stars in our DAV sample have been definitively classified as DAZVs so far, or about 8.5% of the sample. So how do we account for such an obvious discrepancy?

As has been previously stated, we are aware of four DAZVs within the ZZ Ceti instability strip, G29-38, GD133, WD1150-153, and PG 1541+651, each of which hosts a debris disk with an infrared excess (Kilic 2014). From the estimates of Kilic & Redfield (2007) and Barber et al. (2014), only a few percent of DAVs actually have detectable debris disks, which is more closely in line with the fraction represented by our DAZV sample. But the implication remains that our non-polluted DAV sample is likely contaminated with a significant number of stars that actually belong to the DAZV class.

There are a number of possible explanations for this. Firstly, photospheric metals or infrared disks may simply not have been detected yet for some of these stars; indeed, the literature is rather sparse when it comes to the details of the spectra of most of the stars in our sample beyond the effective temperature and log g inferred from it. And even when stars have been inspected for disks, there is the chance that they might be unusually optically thin or gaseous in nature following the sublimation of tidally disrupted material, rendering them essentially undetectable in the infrared (Debes et al. 2012). Edge effects may also hide some

debris disks, though this effect should be fairly small (Debes et al. 2012).

In any case, the contamination of the normal DAV sample does not help the case of the DAZV and non-polluted DAV samples potentially being asterosiesmologically distinct from each other; the uncertainties are inflated in the case of contamination. A corollary of this is that the true fits of the DAZV population would likely come to more closely resemble the current fits for the non-polluted DAVs, further reinforcing our conclusion.

4.4 Extension to ELMVs?

While considering how we could expand our sample, we became aware of extremely low mass (ELM) white dwarfs ($M < 0.25 M_{\odot}$) that were also variables (ELMVs). Only discovered in the last few years, ELMVs appear to represent an extension of the ZZ Ceti instability strip, and are believed to produce g-mode pulsations in the same manner as the canonical ZZ Ceti DAVs, in addition to lower-amplitude p-mode pulsations, though we will remain focused on the g-modes here (Hermes et al. 2012; 2013a). While studying the literature, we found reference to two ELMV stars that also showed evidence of metal contamination, J1112+1117 and J2228, which we classify as ELMZVs (Hermes et al. 2013a; Hermes et al. 2013b).

J1112+1117 has an effective temperature of 9590 K and log g = 6.36 as estimated with the $ML2/\alpha = 0.8$ formulation of mixing length theory used by Gianninas et al. (Hermes et al. 2013a; Gianninas et al. 2011), which converts to about 9450 K and log g = 6.08 under Tremblay et al.'s 3-D convection corrections

(2013). Calcium lines have been detected in its photosphere and it has five independent g-modes with periods ranging from 1792 seconds to 2855 seconds, far longer than any of the pulsation periods of the DAVs in the canonical ZZ Ceti instability strip. Among these g modes, the main period is about 2259 seconds with an amplitude of 7.49 mma, while the WMP is about 2288 seconds (Hermes et al. 2013a).

In contrast, J2228 has $T_{\rm eff}$ = 7870 K and log g = 6.03 under Gianninas et al.'s $ML2/\alpha = 0.8$ formulation (2011), which becomes about 7860 K and log g = 5.72 when 3-D effects are accounted for (Tremblay et al. 2013). Calcium II K lines are also observed for this star. Three independent pulsation periods have been discovered for its g-modes (Hermes et al. 2013b), and from these the WMP can be calculated to be about 4352 seconds, while the main period is about 4178 seconds and has an amplitude of 6.26 mma.

We plot log g versus temperature for these stars, along with three other ELMVs that lack metal pollution and our existing DAV samples, in Figure 8, which is an extension of Figure 7 into the ELM regime. From this figure, we see that the ELMS have lower effective temperatures than their more massive counterparts, though there is clearly significant scatter in this relationship, possibly from the varying cooling ages of the stars.

We can also revisit our fits for WMP and main period versus effective temperature, this time accounting for ELMs, and do so in Figures 9 and 10 and Equations 14 and 15 below, respectively.

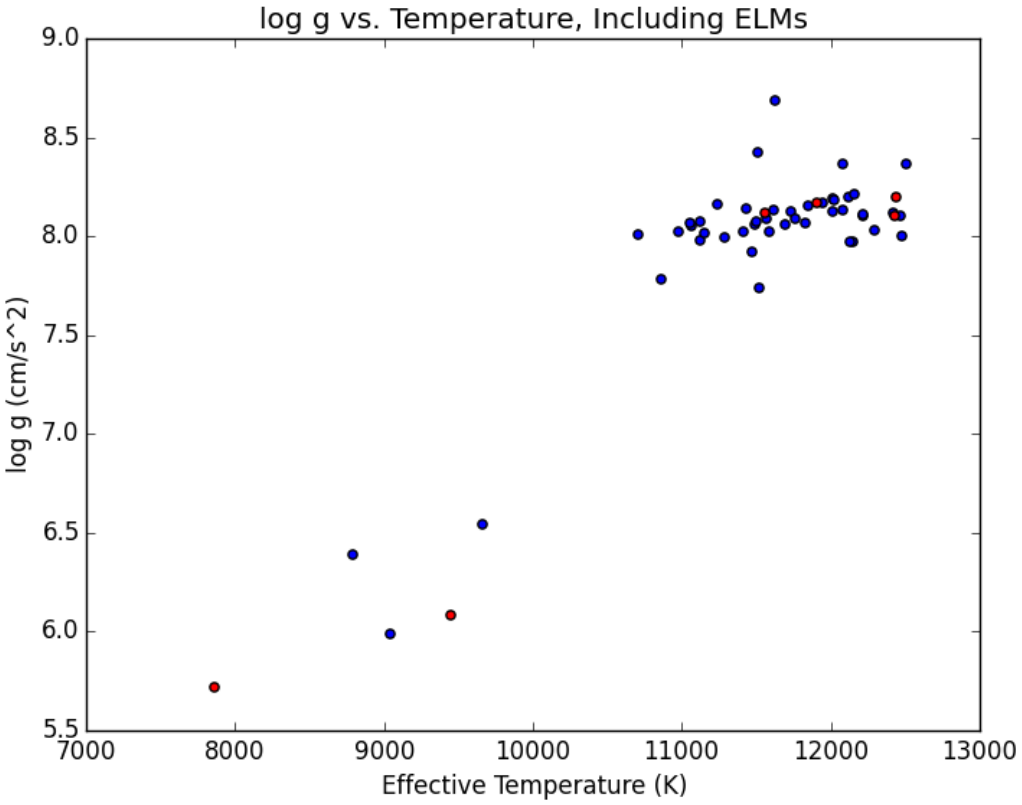

Figure 8: log g vs. effective temperature. The DAZVs are in red, while other DAVs are in blue. ELMs have been added to the plot, and appear in its lower left corner.

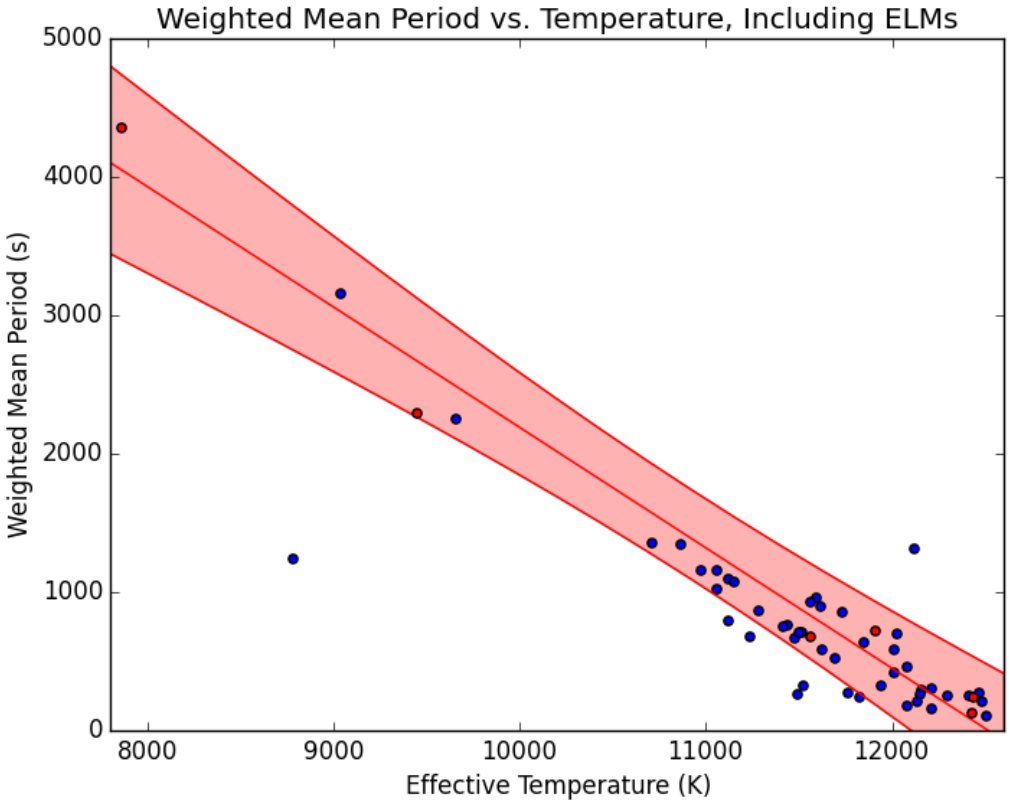

Figure 9: WMP vs. effective temperature, with the ELMV population included. Metal-polluted stars are red, while those that lack known metal pollution are blue.

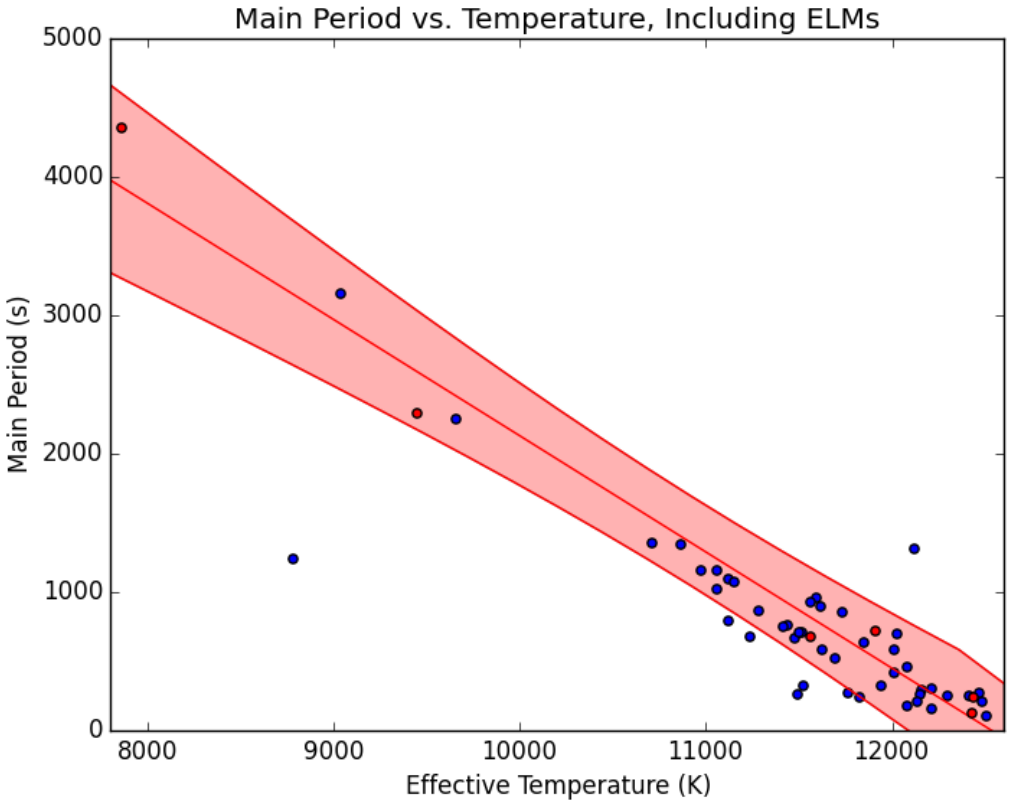

Figure 10: Main Period vs. effective temperature, with the ELMV population included. Metal-polluted stars are red, while those that lack known metal pollution are blue.

$$\mathrm{WMP_{DAZV}} \approx (-0.87 \pm 0.07)\mathrm{T_{eff}} + (10890 \pm 760) \tag{14}$$

$$\mathrm{P_{DAZV}} = (-0.84 \pm 0.06)\mathrm{T_{eff}} + (10530 \pm 640) \tag{15}$$

Here, we see that asterosiesmic behavior of the canonical ZZ Ceti instability strip also seems to extend into the ELM regime as suggested by Hermes et al. (2013b). Far more interestingly, the addition of just two data points has drastically improved the uncertainties in the DAZV fits, and hypothesis testing shows that the slope is now very significantly non-zero, with $p \approx 0.0002$. The slopes are also steeper than before and the intercepts are higher, and are no longer in agreement with the old fits for stars lacking metal pollution.

But we cannot just declare victory with this. We have not directly considered how the fits for the stars lacking metal pollution changes with the addition of the ELMs, and when we do we see that there is an outlier in the ELM regime. Granted, the other two such stars in the ELM regime fall closely along what we could extrapolate from the normal-mass population, but given the paucity of data, it seemed imprudent to assign a fit line here, as the true scatter in this regime could be significantly larger or smaller than what we had observed, or there could be more stars around the apparent outlier hitherto unknown to us which could drastically change the fit. Thus, we reserve judgment in the ELM regime for now; more ELMVs are required for definitive results.

5 Conclusions

Ultimately, we find a null result for the hypothesis that metal-polluted DAZVs might have significantly different asteroseismic properties than non-metal polluted DAVs. A larger sample size of DAZVs must be built up to reduce the relevant uncertainties in the data before a stronger conclusion can be reached, along with a more thorough investigation into possible contamination of the non-polluted DAV sample. The ELM regime may also prove a fruitful area to extend this study into and yield further DAZV candidates.

References

Barber, S.D., et al. 2014 "Dusty WDs in the WISE ALL Sky Survey ∩ SDSS". The Astrophysical Journal, Vol. 786: 77 (6 pp).

Bell, K. 2015. Personal Communications.

Bergeron, P. et al. 2004. "On the Purity of the ZZ Ceti Instability Strip: Discovery of More Pulsating DA White Dwarfs on the Basis of Optical Spectroscopy." The Astrophysical Journal, Vol. 600: 400-408.

Brickhill, A.J. 1991. "The Pulsations of ZZ Ceti Stars - III. The Driving Mechanism." Monthly Notices of the Royal Astronomical Society, Vol. 251, 673-680.

Carroll, B.W. & Ostlie, D.A. 2007. "An Introduction to Modern Astrophysics." 2nd Edition. Pearson: Addison-Wesley. 495-498.

Castanheira, B.G. 2014. Personal Communications.

Castanheira, B.G., et al. 2013. "Discovery of Five New Massive Pulsating White Dwarf Stars." Monthly Notices of the Royal Astronomical Society, Vol. 430: 50-59.

Castanheira, B.G., et al. 2010. "New Developments of the ZZ Ceti Instability Strip: The Discovery of 11 New Variables." Monthly Notices of the Royal Astronomical Society, Vol. 405: 2561-2569.

Debes, J.H., et al. 2012. "Detection of Weak Circumstellar Gas Around the DAZ White Dwarf WD 1124-293: Evidence for the Accretion of Multiple Asteroids." The Astrophysical Journal, Vol. 754: 59 (11 pp).

Gianninas, A., Bergeron, P., & Fontaine, G. 2005. "Toward an Empirical Determination of the ZZ Ceti Instability Strip." The Astrophysical Journal, Vol. 631: 1100-1112.

Gianninas, A, Bergeron, P., and Ruiz, M.T. 2011. " A Spectroscopic Survey and Analysis of Bright, Hydrogen-Rich White Dwarfs." The Astrophysical Journal, Vol. 743: 138 (27 pp).

Graham, J.R., et al. 1990. "The Infrared Excess of G29-38: A Brown Dwarf or Dust?" The Astrophysical Journal, Vol. 357: 216-223.

Green, R.F. , Schmidt, M., & Liebert, J. 1986. "The Palmoar-Green Catalog of Ultraviolet-Excess Stellar Objects." The Astrophysical Journal Supplement Series, Vol. 61: 305-352.

Hermes, J.J., et al. 2013a."Discovery of Pulsations, Including Possible Pressure Modes, In Two New Extremeley Low Mass, He-Core White Dwarfs." The Astrophysical Journal, Vol. 765: 102.

Hermes, J.J., et al. 2013b. "A New Class of Pulsating White Dwarf of Extremely Low Mass: The Foruth and Fifth Members." Monthly Notices of the Royal Astronomical Society: 000, 000-000.

Hermes, J.J., et al. 2012 "SDSS J184037.78+642312.3: The First Pulsating Extremely Low Mass White Dwarf." The Astrophysical Journal Letters, Vol. 750: L28 (5pp).

Jura, M. 2008. "Pollution of Single White Dwarfs By Accretion of Many Small Asteroids." The Astronomical Journal, Vol. 135: 1785-1792.

Jura, M. 2012. "The Elemental Compositions of Extrasolar Plantesimals." Formation, Detection and Characterization of Extrasolar Habitable Planets. Proceedings of the IAU Symposium No. 293.

Kepler, S.O., et al. 1995. "Non-Variable Stars Inside the ZZ Ceti Instability Strip". Baltic Astronomy, Vol. 4: 157-165.

Kilic, M. 2014. Personal Communications.

Kilic, M., et al. 2012. "The Discovery of a Debris Disc Around the DAV White Dwarf PG 1541+651." Monthly Notices of the Royal Astronomical Society, Vol. 419: L59-L63.

Kilic, M. & Redfield, S. 2007. "A Dusty Disk Around WD 1150-153: Explaining the Metals in White Dwarfs By Accretion from the Interstellar Medium Versus Debris Disks." The Astrophysical Journal, Vol. 660: 641-650.

Kilic, M., et al. 2006. " Debris Disks Around White Dwarfs: The DAZ Connection." The Astrophysical Journal, Vol. 646: 474-479.

Kleinman, S.J. 1995. "G 29-38 And Asterosiesmology of the Cool DAV White Dwarfs." Baltic Astronomy, Vol. 4: 270-301.

Kleinman, S.J., et al. 2013. "SDSS DR7 White Dwarf Catalog." The Astrophysical Journal Supplement Series, Vol. 204: 5 (14 pp).

Koester, D. & Allard, N.F. 2000. "The ZZ Ceti Instability Strip Revisited." Baltic Astronomy, Vol. 9: 119-124.

Koester, D., Provencal, J., & Shipman, H.L. 1997. "Metals in the Variable DA G29-38". Astronomy & Astrophysics, Vol. 230: L57-L59.

Koester, D., & Voss, B. 2007. "Six New ZZ Ceti Stars from the SPY and the HQS Surveys." 15th European Workshop on White Dwarfs. ASP Conference Series, Vol. 372: 583-586.

Koester, D. & Wilken, D. 2006. "The Accretion-Diffusion Scenario For Metals in Cool White Dwarfs." Astronomy & Astropysics, Vol. 453: 1051-1057.

Koester, D., et al. 2005. "DAZ White Dwarfs in the SPY Sample." ASP Conference Series, Vol. 334.

Koester, D., et al. 2014. "The Frequency of Planetary Debris Around Young White Dwarfs." Astronomy and Astrophysics, Vol. 566: A34 (20 pp).

Landolt, A.U. 1968. "A New Short-Period Blue Variable*." The Astrophysical Journal, Vol. 153, 151-164.

McCook, G.P. & Sion, E.M. 1999. "A Catalog of Spectoscopically Identified White Dwarfs." Astrophysical Journal Supplement Series, Vol. 121:1-130.

McGraw, J.T. & Robinson, E.L. 1975. "G29-38 and G38-29: Two New Large-Amplitude Variable White Dwarfs." The Astrophysical Journal, Vol. 200: L89-L93.

Mukadam, A.S., et al. 2006. "Ensemble Characteristics of the ZZ Ceti Stars." The Astrophysical Journal, Vol. 640: 956-965.

Princeton Instruments. 2012. "ProEM EMCCD Camera System." Version 1.C.

Shulov, O.S. & Kopatskaya, E.N. 1974. Astrofizika, Vol. 10 (English Translation): 72-74.

Silvotti, R., et al. 2006. "The ZZ Ceti Instability Strip as Seen by

VLT-ULTRACAM." Memorie Scientia Astronomica Italiana, Vol. 77: 486-487.

Strickland, Willie. 2014. Personal Communications.

Tremblay, P.-E. et al. 2013. " Spectroscopic Analysis of DA White Dwarfs with 3D Model Atmospheres." Astronomy and Astrophysics, Vol. 559: A104 (23 pp).

Tremblay, P.-E. et al. 2010. "New Insights into the Surface Gravity Distribution of Cool DA White Dwarfs." The Astrophysical Journal, Vol. 712: 1345-1358.

Tremblay, P.-E. & Bergeron, P. 2009. "Spectroscopic Analysis of DA White Dwarfs: Stark Broadening of Hydrogen Lines Including Nonideal Effects." The Astrophysical Journal, Vol. 696: 1755-1770.

Vauclair, G., et al. 2000. "PG 1541+650: A New ZZ Ceti White Dwarf." Baltic Astronomy, Vol. 8: 133-140.

Xu, S., et al. 2014. "Elemental Composition of Two Extrasolar Rocky Planetesimals." The Astrophysical Journal, Vol. 783:79 (16 pp).

Zuckerman, B., et al. 2010. "Ancient Planetary Systems Are Orbiting a Large Fraction of White Dwarf Stars." The Astrophysical Journal, Vol. 722: 725-736.

Zuckerman, B. & Becklin, EE. 1987. "Excess Infrared Radiation from a White Dwarf - An Orbiting Brown Dwarf?" Nature, Vol. 300: 138-149.

Zuckerman, B. et al. 2003. "Metal Lines in DA White Dwarfs." The Astrophysical Journal, Vol. 596: 477-495.